J Supercond Nov Magn (2014) 27:421–425
DOI 10.1007/s10948-013-2278-1

ORIGINAL PAPER

# Magnetocaloric Effect in Different Impurity Doped $La_{0.67}Ca_{0.33}MnO_3$ Composite

**R. M'nassri · A. Cheikhrouhou**

Received: 3 June 2013 / Accepted: 5 June 2013 / Published online: 22 June 2013


**Abstract** In this paper, we investigate the effect of nonmagnetic YSZ and magnetic $Fe_3O_4$ addition on the magnetocaloric properties of the $La_{0.67}Ca_{0.33}MnO_3$ composite. The temperature dependences of the magnetization for pure LCMO and the impurity doped LCMO composite upon 0.1, 0.3, and 1 T magnetic field were simulated. By the help of the phenomenological model, magnetic entropy change and specific heat for magnetic field variation are predicted. The values of maximum magnetic entropy change, full-width at half-maximum, and relative cooling power were calculated at several magnetic fields. The $\Delta S_M$ value is 2.45, 2.39, and 5.58 J kg$^{-1}$ K$^{-1}$ at 1 T for pristine LCMO, LCMO/YSZ, and LCMO/$Fe_3O_4$, respectively.

**Keywords** Model · Manganites · Composites · Magnetization · Magnetic entropy change · Heat capacity change

## 1 Introduction

The magnetocaloric effect (MCE) is a property common to all magnetic materials [1]. It is associated with the magnetic entropy change ($\Delta S_M$) that occurs due to a change in an applied magnetic field. This effect is the basis of magnetic refrigeration technology, which promises efficient and environmentally friendly green technology to substitute common vapor-cycle based ones [2, 3]. Since the discovery of the giant MCE in GdGeSi at Ames Laboratory [4], the research on magnetic refrigerant materials has been strongly intensified worldwide. Currently, most research groups study the MCE in rare-earth-based materials because the large moments of the rare-earth atoms imply the possibility of large MCE [5–8]. Rare-earth perovskite manganites of the general formula $La_{1-x}Ca_xMnO_3$ have attracted much attention because of their higher potential for magnetic sensor applications based on the magnetoresistance effect. Several researchers have attempted to enhance the CMR effect of manganites by making composites of these materials with secondary phases [9–13]. Additionally, these materials are very convenient for the preparation routes, and their Curie temperature can be justified under the various doping conditions. Therefore, the new trends have been focusing on studying the MCE of manganite composite [14–16]. Due to the large $\Delta S_M$, they have been widely used for magnetic refrigeration applications in different temperature ranges.

In this paper, we present the effect of nonmagnetic YSZ and magnetic $Fe_3O_4$ dopant on magnetocaloric properties in $La_{0.67}Ca_{0.33}MnO_3$ composite. A pure LCMO prepared by sol-gel method and mixed with YSZ and $Fe_3O_4$ according to the nominal formula $(1-x)La_{0.67}Ca_{0.33}MnO_3 + x$YSZ (or $Fe_3O_4$), where YSZ represents yttria-stabilized zirconia and the doping level of both YSZ and $Fe_3O_4$ is 1 mol% [17]. Using the phenomenological model for simulation of the variation of the magnetization with temperature, the magnetocaloric properties such as magnetic entropy change, heat capacity change, and relative cooling power were predicted.

## 2 Model Calculations

Within the phenomenological model, described in [18], the variation of the magnetization with temperature is repre-

R. M'nassri (✉) · A. Cheikhrouhou
Laboratoire de Physique des Matériaux, Faculté des Sciences de Sfax, Sfax University, B.P. 1171, 3000 Sfax, Tunisia
e-mail: rafik_mnassri@yahoo.fr

A. Cheikhrouhou
Institut NEEL, B.P. 166, 38042 Grenoble Cedex 9, France

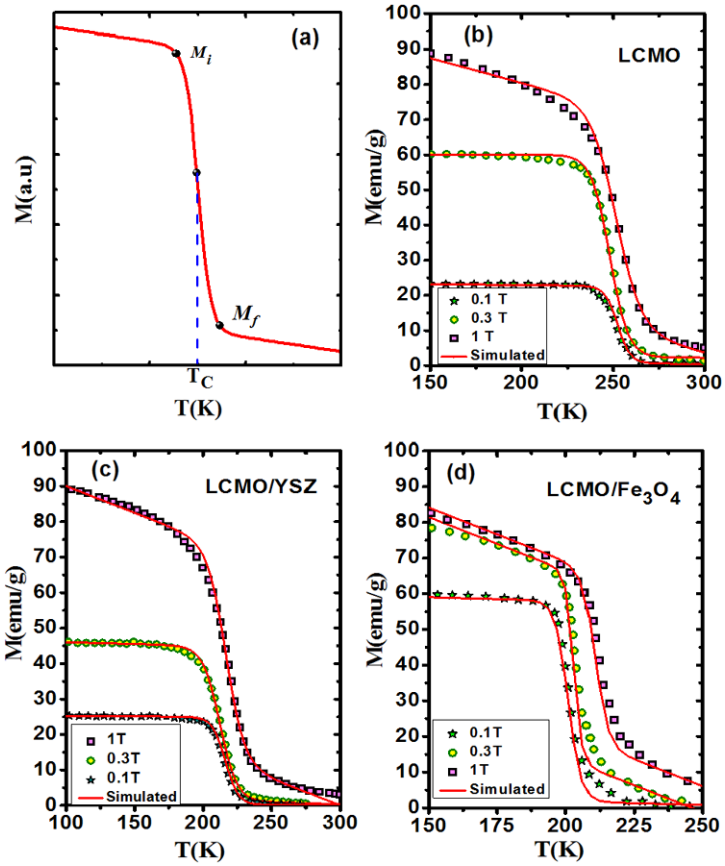


**Fig. 1** (**a**) Temperature dependence of magnetization in constant applied magnetic field. (**b**), (**c**), and (**d**) Magnetization for the LCMO, LCMO/YSZ, and LCMO/$Fe_3O_4$ versus temperature at several magnetic fields. The *solid lines* are modeled results and symbols represent experimental data from [17]

sented by

$$M(T, H = H_{\max}) = \left(\frac{M_i - M_f}{2}\right)\left[\tanh\left(A(T_C - T)\right)\right] + BT + C \quad (1)$$

where $H_{\max}$ is the maximum external field, $T_C$ is a Curie temperature, $M_i$ ($M_f$) is an initial (final) value of magnetization at ferromagnetic–paramagnetic transition as shown in Fig. 1a. Here, $A = 2(\frac{B - S_c}{M_i - M_f})$, $B$ magnetization sensitivity $dM/dT$ at ferromagnetic state before transition, $S_c$ is magnetization sensitivity $dM/dT$ at $T_C$, and $C = (\frac{M_i - M_f}{2}) - BT_C$.

The $\Delta S$ can be obtained through the adiabatic change of temperature by the application of a magnetic field. A $\Delta S$ as a function of temperature for a field variation from 0 to $H_{\max}$ is given by

$$\Delta S(T, \Delta H = H_{\max}) = H_{\max}\left[-A\left(\frac{M_i - M_f}{2}\right)\operatorname{sech}^2\left(A(T_C - T)\right) + B\right] \quad (2)$$

A more abrupt variation of magnetization near the magnetic transition occurs and results in a large magnetic entropy change. $\Delta S$ depends on the temperature gradient of the magnetization and reaches a maximum value around $T_C$.

Relative cooling power is a useful parameter, which decides the efficiency of magnetocaloric materials based on the magnetic entropy change [19, 20]. The RCP is defined as the product of the maximum magnetic entropy change $\Delta S_{M\max}$ and full width at half- maximum in $\Delta S_M(T)$ curve ($\delta T_{\mathrm{FWHM}}$). According to this model [18], $\Delta S_{M\max}$ is available by

$$\Delta S_{M\max} = H_{\max}\left[-A\left(\frac{M_i - M_f}{2}\right) + B\right] \quad (3)$$

and $\delta T_{\mathrm{FWHM}}$ is presented by

$$\delta T_{\mathrm{FWHM}} = \frac{2}{A}\cosh^{-1}\left(\frac{2A(M_i - M_f)}{A(M_i - M_f) + 2B}\right)^{1/2} \quad (4)$$

The RCP is computed by

$$RCP = -\Delta S_{M\max}\delta T_{\mathrm{FWHM}} = H_{\max}\left(M_i - M_f - \frac{2B}{A}\right) \times \cosh^{-1}\left(\frac{2A(M_i - M_f)}{A(M_i - M_f) + 2B}\right)^{1/2} \quad (5)$$

The RCP corresponds to the amount of heat that can be transferred between the cold and hot parts of the refrigerator

**Table 1** Model parameters for LCMO, LCMO/YSZ, and LCMO/$Fe_3O_4$

| Material | $\mu_0 H$ (T) | $M_i$ (emu/g) | $M_f$ (emu/g) | $T_C$ (K) | $B$ (emu/g K) | $S_C$ (emu/g K) |
|---|---|---|---|---|---|---|
| $La_{0.67}Ca_{0.33}MnO_3$ | 0.1 | 22.6549 | 0.70796 | 252.347 | −0.005 | −1.61792 |
| | 0.3 | 60 | 2.30088 | 248.042 | −0.001 | −2.93283 |
| | 1 | 73.2743 | 10.4425 | 251.569 | −0.14 | −2.45106 |
| LCMO/YSZ | 0.1 | 25.0341 | 0.19267 | 216.275 | −0.001 | −1.30301 |
| | 0.3 | 44.8908 | 1.25709 | 212.334 | −0.01 | −1.77544 |
| | 1 | 72.4718 | 12.5159 | 216.79217 | −0.15 | −2.39306 |
| LCMO/$Fe_3O_4$ | 0.1 | 57.9883 | 1.80283 | 201.043 | −0.02 | −6.12067 |
| | 0.3 | 65.5538 | 12.9024 | 203.08735 | −0.3 | −9.78289 |
| | 1 | 65.9028 | 17.8265 | 210.79191 | −0.3 | −5.58148 |

in one ideal thermodynamic cycle. This parameter allows an easy comparison of different magnetic materials for applications in magnetic refrigeration; hence, larger RCP values lead to better magnetocaloric materials.

The heat capacity can be calculated from the magnetic contribution to the entropy change induced in the material, $\Delta C_{P,H}$, by the following expression:

$$\Delta C_{P,H} = T\frac{\partial \Delta S_M}{\partial T} \tag{6}$$

From this model [18], a determination of $\Delta C_{P,H}$ can be carried out as follows:

$$\Delta C_{P,H} = H_{\max}\big[-T A^2(M_i - M_f) \times \operatorname{sech}^2\big(A(T_C - T)\big)\tanh\big(A(T_C - T)\big)\big] \tag{7}$$

## 3 Simulation

Five parameters can be used to apply the model [18]. $M_i$, $M_f$, and $T_C$ parameters were obtained by experimental data in Fig. 1(a) and calculation of magnetization sensitivity at both $T_C$ and ferromagnetic state before transition (Sc and B), as displayed in Table 1. Figure 1(b), (c), and (d) show temperature dependences of the magnetization for pure LCMO and the impurity doped LCMO composite upon 0.1, 0.3, and 1 T magnetic fields. The symbols represent experimental data from [17] while the solid line represents modeled data using parameters given in Table 1. The results of calculations and experimental data of magnetization are in good agreement for the composites.

The large magnetocaloric effect in manganites mainly originates from the considerable variation of magnetization near $T_C$ [7]. The strong coupling between spin and lattice plays an important role in the magnetic ordering process [21]. In order to understand the influence of the YSZ and $Fe_3O_4$ dopant, the magnetic entropy change and heat capacity of the composites have been derived from the simulated magnetization on the basis of Eq. (3) and Eq. (7). respectively. The modeled results for field changes from 0 to 0.1, 0 to 0.3, and 0 to 1 T are shown in Fig. 2 for all materials. The $\Delta S_{M\max}$ value is 2.45, 2.39, and 5.58 $\mathrm{J\,kg^{-1}K^{-1}}$ at 1 T for pristine LCMO, LCMO/YSZ, and LCMO/$Fe_3O_4$, respectively.

The maximum of the magnetic entropy change, full-width at half-maximum, and RCP predicted for composites at several magnetic fields are listed in Table 2. Table 2 summarizes the reported values of magnetic and magnetocaloric parameters obtained by different authors, along with the present data.

As the Fig. 2 shows, anomalies are observed in all curves around $T_C$, which are due to the magnetic phase transition. The value of $\Delta C_{P,H}$ changes suddenly from positive to negative around $T_C$ and rapidly decreases with decreasing temperature. Furthermore, the maximum and minimum values of $\Delta C_{P,H}$ for each sample are determined from Fig. 2 and listed in Table 2.

According to the results, the $\Delta S$ and $\Delta C_{P,H}$ have been affected by the doped impurities. The doped YSZ ($Fe_3O_4$) as a second phase are located mainly at the grain boundaries and/or surfaces of LCMO grains [17]. It is illustrated that Mn spin disorders at the phase interfaces due to which Mn–Mn magnetic exchange is interrupted due to YSZ (or $Fe_3O_4$) segregation at the grain boundaries. Due to its very important resistivity [22], a nonmagnetic impurity YSZ for could act as obstacles for the formation of ferromagnetic domains. For the LCMO/$Fe_3O_4$, a deviation is seen from the change of the magnetization curve, which may be attributed to the existence of a new magnetic domain related to $Fe_3O_4$. It is reported that the magnetic $Fe_3O_4$ is related to the improvement of the magnetic homogeneity of the specimens and improves ferromagnetic in nonmagnetic intergrain region. A magnetic impurity is able to participate in the formation of ferromagnetic ordering [22]. With the application of an external magnetic field, the disordered spins can align with each other, as a result producing the large $\Delta M$, hence, large $\Delta S$ at low magnetic field.

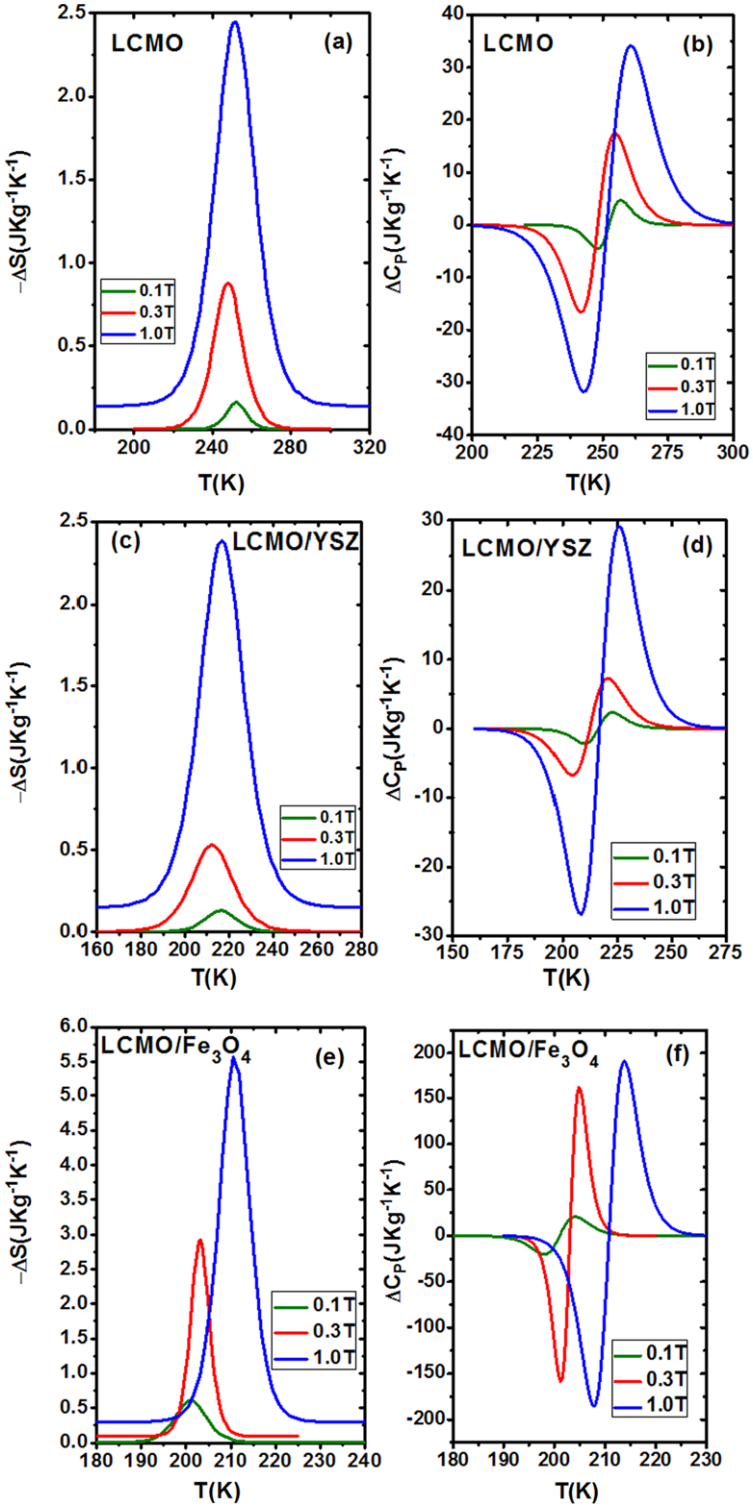


**Fig. 2** Magnetic entropy change and the heat capacity change for: (**a**) and (**b**) LCMO, (**c**) and (**d**) LCMO/YSZ, and (**e**) and (**f**) LCMO/$Fe_3O_4$

## 4 Conclusion

In conclusion, the magnetocaloric response of different impurity $La_{0.67}Ca_{0.33}MnO_3$ composite has been predicted. Improvements in magnetocaloric properties have been observed with $Fe_3O_4$ addition in polycrystalline manganites. This result is very important for practical applications because lower fields like 0.1, 0.3, 1 T are much easier to generate by permanent magnets than higher fields like 2 T. So, this model is useful for the development of refrigeration devices and evaluation of its efficiency. We hope this study can stimulate the synthesis and characterization of composites in

**Table 2** Comparison of maximum entropy change, specific heat change and RCP for $La_{0.67}Ca_{0.33}MnO_3$-based materials and several materials

| Material | $\mu_0 H$ (T) | $\Delta S_{max}$ ($J\,kg^{-1}\,K^{-1}$) | $\delta T_{FWHM}$ (K) | $RCP$ ($J\,kg^{-1}$) | $\Delta C_{P,H\,min}$ ($J\,kg^{-1}\,K^{-1}$) | $\Delta C_{P,H\,max}$ ($J\,kg^{-1}\,K^{-1}$) | Ref. |
|---|---|---|---|---|---|---|---|
| $La_{0.67}Ca_{0.33}MnO_3$ | 0.1 | 0.16179 | 12.0227 | 1.94517 | −4.523507 | 4.685379 | Present |
| | 0.3 | 0.87985 | 17.35037 | 15.26572 | −16.60219 | 17.512868 | Present |
| | 1 | 2.45106 | 25.1458 | 61.63385 | −31.71127 | 34.100551 | Present |
| $La_{0.67}Ca_{0.33}MnO_3$ (solid–solid) | 3 | 6.4 | 20.937 | 134 | – | – | [23] |
| $La_{0.67}Ca_{0.33}MnO_3$ (solid–solid) | 1.5 | 4.3 | 10.93 | 47 | – | – | [21] |
| $La_{0.67}Ca_{0.33}MnO_3$ thin film | 5 | 2.06 | 84.951 | 175 | – | – | [24] |
| LCMO/YSZ | 0.1 | 0.1303 | 16.82631 | 2.19249 | −2.199216 | 2.3323561 | Present |
| | 0.3 | 0.53263 | 21.8827 | 11.65538 | −6.719179 | 7.2764329 | Present |
| | 1 | 2.39306 | 24.84545 | 59.45668 | −26.85782 | 29.119269 | Present |
| LCMO/$Fe_3O_4$ | 0.1 | 0.61207 | 8.13857 | 4.98135 | −20.14805 | 20.761541 | Present |
| | 0.3 | 2.93487 | 5.01883 | 14.7296 | −158.6344 | 161.40222 | Present |
| | 1 | 5.58148 | 8.39413 | 46.85171 | −185.5947 | 190.96898 | Present |
| $Pr_{2/3}Ba_{1/3}MnO_3$/PdO | 5 | 3.4523 | – | 147.8762 | – | – | [14] |
| $La_{0.7}Ca_{0.2}Sr_{0.1}MnO_3$/Ag | 5 | 7.6 | – | – | – | – | [15] |
| 1/m LKMO/Ag ($m = 32$) | 1 | 1.86 | – | – | – | – | [16] |

this series as well as many others in order to check our predictions.

**Acknowledgements** This study was supported by the Tunisian Ministry of Higher Education and Scientific Research.

## References

1. Tishin, A.M., Spichkin, Y.I.: The magnetocaloric effect and its applications. Institute of Physics (2003)
2. Bruck, E.: J. Phys. D, Appl. Phys. **38**, R381 (2005)
3. Phan, M.H., Yu, S.C.: J. Magn. Magn. Mater. **308**, 325 (2007)
4. Pecharsky, V.K., Gschneidner, K.A. Jr.: Phys. Rev. Lett. **78**, 4494 (1997)
5. Hamad, M.A.: Mater. Lett. **82**, 181–183 (2012)
6. M'nassri, R., Cheikhrouhou-Koubaa, W., Koubaa, M., Boudjada, N., Cheikhrouhou, A.: Solid State Commun. **151**, 1579 (2011)
7. M'nassri, R., Cheikhrouhou-Koubaa, W., Chniba-Boudjada, N., Cheikhrouhou, A.: J. Appl. Phys. **113**, 073905 (2013)
8. M'nassri, R., Cheikhrouhou-Koubaa, W., Boudjada, N., Cheikhrouhou, A.: J. Supercond. Nov. Magn. **26**, 1429 (2013)
9. Siwacha, P.K., Srivastav, P., Singh, J., Singh, H.K., Srivastava, O.N.: J. Alloys Compd. **481**, 17 (2009)
10. Lu, W.J., Sun, Y.P., Zhu, X.B., Song, W.H., Du, J.J.: Mater. Lett. **60**, 3207 (2006)
11. Xia, Z.C., Yuan, S.L., Feng, W., Zhang, L.J., Zhang, G.H., Tang, J., Liu, L., Liu, S., Peng, G., Niu, D.W., Chen, L., Zheng, Q.H., Fang, Z.H., Tang, C.Q.: Solid State Commun. **128**, 291 (2003)
12. Xia, Z.C., Yuan, S.L., Zhang, G.H., Zhang, L.J.: J. Phys. D, Appl. Phys. **36**, 217 (2003)
13. Anurag, G., Varma, G.D.: J. Alloys Compd. **453**, 423 (2008)
14. Panwar, N., Coondoo, I., Agarwal, S.K.: J Mater. Lett. **64**, 2638–2640 (2010)
15. Jha, R., Kumar Singh, S., Kumar, A., Awana, V.P.S.: J. Magn. Magn. Mater. **324**, 2849–2853 (2012)
16. Jian, W.: J. Magn. Magn. Mater. **476**, 859–863 (2009)
17. Xia, Z.C., Yuan, S.L., Feng, W., Zhang, L.J., Zhang, G.H., Tang, J., Liu, L., Liu, D.W., Zheng, Q.H., Chen, L., Fang, Z.H., Liu, S., Tang, C.Q.: Solid State Commun. **127**, 567–572 (2003)
18. Hamad, M.A.: Phase Transit. **85**, 106–112 (2012)
19. Pecharsky, V.K., Gschneidner, K.A., Tsokol, A.O.: Rep. Prog. Phys. **68**, 1479 (2005)
20. Gschneidner, K.A. Jr., Pecharsky, V.K.: Annu. Rev. Mater. Sci. **30**, 387 (2000)
21. Guo, Z.B., Du, Y.W., Zhu, J.S., Huang, H., Ding, W.P., Feng, D.: Phys. Rev. Lett. **78**, 1142 (1997)
22. Xia, Z.C., Yuan, S.L., Feng, W., Zhang, L.J., Zhang, G.H., Tang, J., Cheng, L., Zheng, Q.H., Liu, L., Liu, S., Tang, C.Q.: Solid State Comm **126**, 567–571 (2003)
23. Sun, Y., Xu, X., Zhang, Y.H.: J. Magn. Magn. Mater. **219**, 183 (2000)
24. Morelli, D.T., Mance, A.M., Mantese, J.V., Micheli, A.L.: J. Appl. Phys. **79**, 373 (1996)